THE DELAMINATION EFFECTS ON THE IMPACT RESISTANCE OF SINGLY CURVED COMPOSITE SHELLS

N. O. Yokoyama, yokoyama@ita.br
M. V. Donadon, donadon@ita.br
Intituto Tecnológico de Aeronáutica – ITA

S. F. M. de Almeida, frascino@ita.br
Intituto Tecnológido de Aeronáutica - ITA

Abstract. This paper presents a numerical study of the delamination effects on the impact resistance of composite laminates with three different curvatures. The numerical simulations were performed on ABAQUS 6.5-1 by using a non-linear three-dimensional damage model proposed by Donadon. The damage model includes irreversible strains, shear non-linearities and strain rate effects. The delamination effects were simulated by using an interface layer of cohesive material placed at the midplane of the laminate. Also, simulations without considering the cohesive layer were carried out for comparison purposes. The results indicated that the delamination has a great influence on the impact resistance of singly curved composite laminates.

Keywords*:* Delamination, Impact, Composite Laminates

1. INTRODUCTION

Composite laminates subjeted to impact load are susceptible to delamination. This failure mode, unlike the other failure modes, only can be represented numerically by using solid elements. Sun and Jih (1995) investigated the quasi-static characteristics of impact-induced delamination crack propagation in graphite/epoxy laminates. In their study cross-ply laminates subjected to low-velocity heavy mass impact have been investigated. A spring-mass model based on the static deflection was used to predicted the contact force history and showed a good agreement with experimental results. Besides the delamination, geometric properties also can influence on the impact resistance of composite laminates. Yokoyama et al (2010) analysed numerically the impact resistance of composite laminates with different curvatures. In order to evaluated the impact induced damage on the structural response of the laminates, a damage model based on Continuum Damage Mechanics and fracture mechanics approaches for shell elements was implemented into ABAQUS 6.5-1 FE code.

Gning et al (2005) studied experimentally the damage progression in thick composite tubes under impact loading with velocities range between 1.72m/s and 7.48m/s. The tubes had lay-up $[\pm 55]_{10}$, lamina thickness of 0.302 mm and inside diameter 55mm. Their results showed that above 4J impact energies delaminations occurs and at higher energies these delaminations propagate and interlaminar cracks appears. Olsson (2010) presented an analytical model for delamination growth during small mass impact on plates. His analytical results were validated by using FE simulations using the software LS-DYNA and experimental results. A cohesive layer at the midplane was modelled using solid elements to simulate the delamination growth, which occurred in pure Mode II. The results from his analytical model showed a good agreement with both experimental and numerical results. In this work, impact simlations on singly curved composite plates were carried out and the curvature and delaminatios effects were investigated.

2. DAMAGE MODEL

A non-linear three-dimensional damage model proposed by Donadon et al (2009) was used in this paper. The damage model accounts the irreversible stains, shear non-linearities and strain rate effects by using a viscoplastic damageable constitutive law. The formulation combine stress based, contunuum damage mechanics and fracture mechanics approaches using a smeared cracking formulation.

The model accounts for fibre failure in tension/compression, matrix cracking in tension/compression and in-plane shear cracking by using the following stress based failure criteria,

Fibre failure in tension:

$$\mathrm{F}_1^{\mathrm{t}}\left(\sigma_1\right)=\frac{\sigma_1}{\mathrm{X}_{\mathrm{t}}} \geq 1 \tag{1}$$

Fibre failure in compression:

$$F_1^c(\sigma_1)=\frac{|\sigma_1|}{X_c}\geq 1 \tag{2}$$

Matrix cracking in tension/shear:

$$F_2^t(\sigma_2,\tau_{23},\tau_{12})=\left(\frac{\sigma_2}{Y_t}\right)^2+\left(\frac{\tau_{23}}{S_{23}}\right)^2+\left(\frac{\tau_{12}}{S_{12}}\right)^2\geq 1 \tag{3}$$

Matrix cracking in compression

$$F_2^c(\sigma_{nn},\tau_{nl},\tau_{nt})=\left(\frac{\tau_{nl}}{S_{23}^A+\mu\sigma_{nn}}\right)^2+\left(\frac{\tau_{nt}}{S_{12}+\mu\sigma_{nn}}\right)^2\geq 1 \tag{4}$$

In-Plane Shear Failure:

$$F_{12}(\tau_{12})=\frac{|\tau_{12}|}{S_{12}}\geq 1 \tag{5}$$

where X_t and X_c are the longitudinal strengths in tension and compression, respectively, Y_t is the transversal strength in tension, S_{12} and S_{23} are the in-plane shear and out-of-plane shear strengths, respectively; σ_{mn}, τ_{nl}, and τ_{nt} are the normal and shear stresses acting on the potential fracture plane (Puck and Shurmmann, 1998). S_{23}^A is the effective shear strength of the material in the potential fracture plane. The criteria of matrix cracking in tension or shear is based on the interactive quadratic failure criterion given by Pinho et al (2006a, 2006b) and the failure criterion for matrix cracking in compression was proposed by Puck and Shurmmann (1998). When one of the criteria presented above is met, damage start to grows according to the linear-polynomial damage evolution law proposed by Donadon et al (2009).

3. DELAMINATION MODELING

The failure modes associated with delamination were modelled using a cohesive model. The cohesive model was implemented into ABAQUS as a user defined material model within solid elements. This model enables the prediction of the mixed mode delamination without knowing *a priory* the mixity ratio between different delamination modes. The modelling of the cohesive layer account for the initiation and propagation criterions as showed on Figure 1.

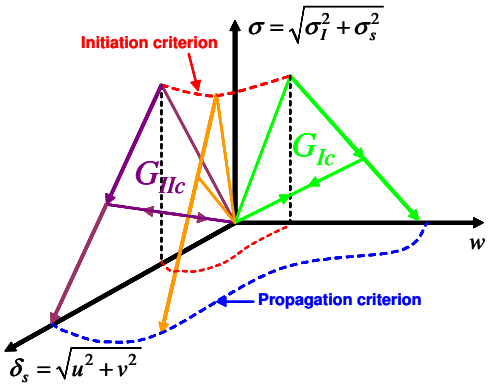

Figure 1. Initiation and propagation criterion

The constitutive law is written in terms of the following relationship between interfacial stresses and interfacial relative displacements,

$$\begin{Bmatrix}\sigma_I\\ \sigma_{II}\\ \sigma_{III}\end{Bmatrix}=\begin{bmatrix}K_I(1-d(\bar{\delta})) & 0 & 0\\ 0 & K_{II}(1-d(\bar{\delta})) & 0\\ 0 & 0 & K_{III}(1-d(\bar{\delta}))\end{bmatrix}\begin{Bmatrix}\delta_I\\ \delta_{II}\\ \delta_{III}\end{Bmatrix} \tag{6}$$

with

$$d(\bar{\delta}) = 1 - \frac{\bar{\delta}_0}{\bar{\delta}}\left[1 + \left(\frac{\bar{\delta} - \bar{\delta}_0}{\bar{\delta}_f - \bar{\delta}_0}\right)^2 \left\{2\left(\frac{\bar{\delta} - \bar{\delta}_0}{\bar{\delta}_f - \bar{\delta}_0}\right) - 3\right\}\right] \tag{7}$$

where K_I, K_{II} and K_{III} are the interfacial stiffnesses associated with mode I, II and III, respectively. σ_I, σ_{II} and σ_{III} are the interfacial stresses and δ_I, δ_{II} and δ_{III} are the respective relative displacements associated with mode I, II and III. $\bar{\delta}_0$ is the equivalent displacement at damage onset obtained from a quadratic stress based criterion. $\bar{\delta}_f$ is the final displacement when damage $d(\bar{\delta})$ =1 and the stresses are equal to zero obtained from the energy based failure criterion. Details on the model formulation may be found in (Donadon and Almeida, 2010).

4. NUMERICAL SIMULATIONS

Impact simulations on composite laminates for different curvatures were carriod out in this paper. Two curvatures have been used: κ_1=0, κ_2=0.008 mm^{-1} and κ_3=0.010 mm^{-1} with a lay-up $[(0/\pm45/90)_2/(0)_2]_s$ and lamina thickness 0.23 mm. The laminates had dimensions of 85 mm × 145 mm × 4.6 mm and the striker has 1.573 g mass and 12.7 mm of diameter. The simulations were performed on ABAQUS by using a non-linear three-dimensional damage model previous described. A cohesive layer (also called interface) placed at the midplane of the laminate was used to simulate the delamination effects. Figure 2 shows the simulations mesh used for plane plate and curved plate for both cases, with and without coheive layer.

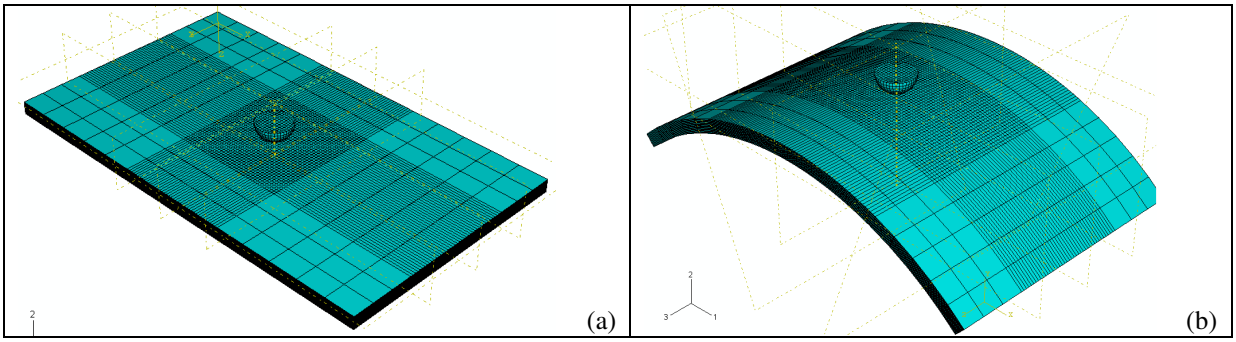

Figure 2. Mesh with solid elements and interface layer for (a) plane and (b) curved plate.

The laminates were assumed to be simply-supported along their edges and the striker has only the displacement on vertical direction free. Solid elements were used for both plate and striker. The contact between striker and plates was defined using the nodal erosion contact available on ABAQUS. The mechanical properties used for the laminate and the cohesive layer are presented in Table 1 and

Table **2**, respectively. Those properties were obtained from the literature and they are representative of carbon/epoxy woven ply laminates. Numerical simulations with impact energies ranging from 2 *J* to 16 *J* were carriod out.

Table 1. Lamina Properties

Mechanical Properties		**Ply Strengths**		**Intralaminar fracture toughnesses**	
E_1 (GPa)	60.8	X_t (MPa)	621	G_f^t (kJ/m^2)	165
$E_2 = E_3$ (GPa)	58.25	X_c (MPa)	760	G_f^c (kJ/m^2)	25
$\nu_{12}=\nu_{13}$	0.07	Y_t (MPa)	594	G_m^t (kJ/m^2)	10
ν_{23}	0.4	Y_c (MPa)	707	G_m^c (kJ/m^2)	2
$G_{12} = G_{13}$ (GPa)	4.55	S_{12} (MPa)	125	G_s (kJ/m^2)	2

Table 2. Cohesive layer (interface) properties

Mechanical properties and ply strengths		Interlaminar fracture toughnesses	
E_3 (GPa)	2.97	G_{IC}	585
$G_{13} = G_{23}$ (MPa)	100	G_{IIC}	2500
$S_{13} = S_{23}$ (MPa)	100	G_{IIIC}	2500

5. RESULTS AND DISCUSSIONS

The results were presented in terms of Contact Force history, Delaminated area, failure modes and dissipated energy for each case. The failure modes were obtained by the damage model and the dissipated energy by the integration of the force-displacement curve. The delamination effects were analysed by the Dissipated Energy × Impact Energy for each plate with and without cohesive layer. Also the delaminated area were compare for each plate in all impact energies studied herein.

Figure 3 shows a comparison between the Dissipated Energy × Impact Energy for the plane plate with and without a cohesive layer at impact energies range from 2 *J* to 16 *J*. The delamination first appears at impact energy of 6 J for the plane plate. The damage for all impact energies was greater for the plate which consider the cohesive layer then for the laminate without cohesive layer, even at impact energies which the delamination not occurs.

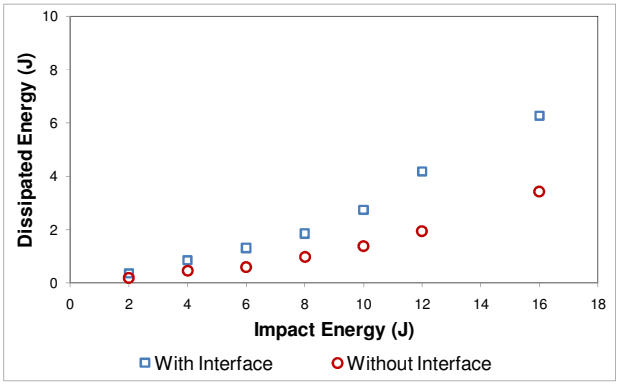

Figure 3. Dissipated Energy × Impact Energy for Plane Plate

Figure 4 shows the Contact Force Time Histories for the impact energy of 4 *J* and 16 *J* comparing the numerical results with and without cohesive layer. At impact energy of 4 J, which does not exhibit delamination, the peak force during the impact loading was similar for both cases. Since the delamination occurs the peak force was lower and the duration of the event was longer for the plate with cohesive layer compared to the plate without cohesive layer, as depicted in Figure 4(b).

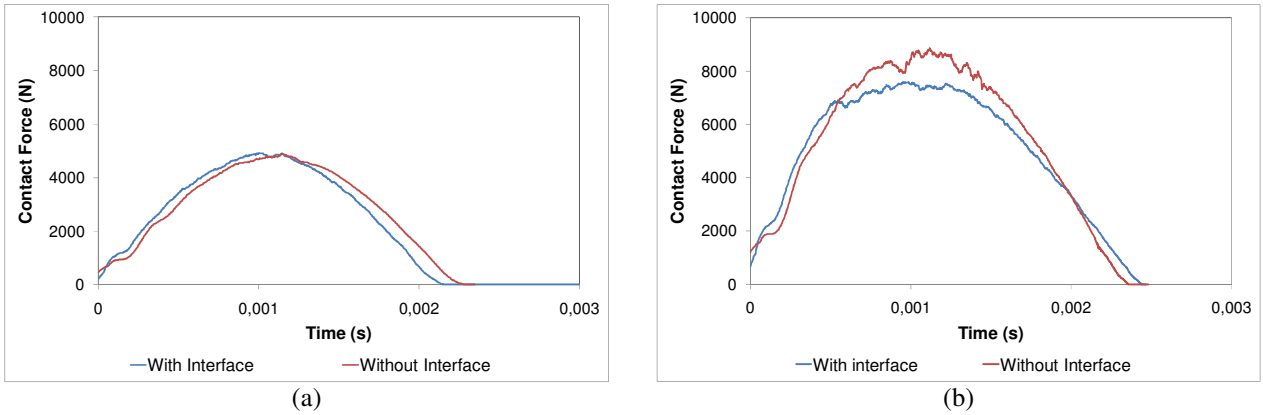

(a) (b)

Figure 4. Contact Force time histories for plane plate at impact energies of (a) 4 *J* and (b) 16 *J*.

A comparison in terms of the dissipated energy between the curved plates with and without cohesive layer is presented in Figure 5. Like for the plane plate the dissipated energy for each impact energy on curved plate was greater for the laminate with cohesive layer and the damage grows with the delamination.

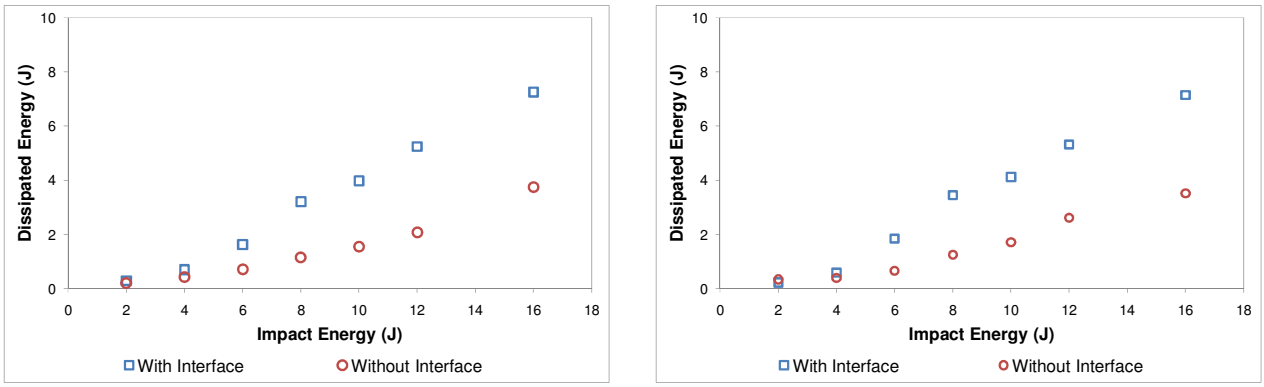

Figure 5. Dissipated Energy × Impact Energy for Curved Plate, (a) κ_2=0.008 mm^{-1} and (b) κ_3=0.010 mm^{-1}

The Contact Force Histories for the curved plate with κ_3=0.010 mm^{-1} is presented in Figure 6 for impact energies of 4 *J* and 16 *J*, with and without consider the cohesive layer. In Figure 6(b) for the impact energiy of 16 *J* the susceptibily of curved plates to delamination effects can be verified in the Contact Force Histories behaviour. Since the delamination occurs the peak force was lower and the event duration was longer for the laminate with cohesive layer compared to the laminate without cohesive layer.

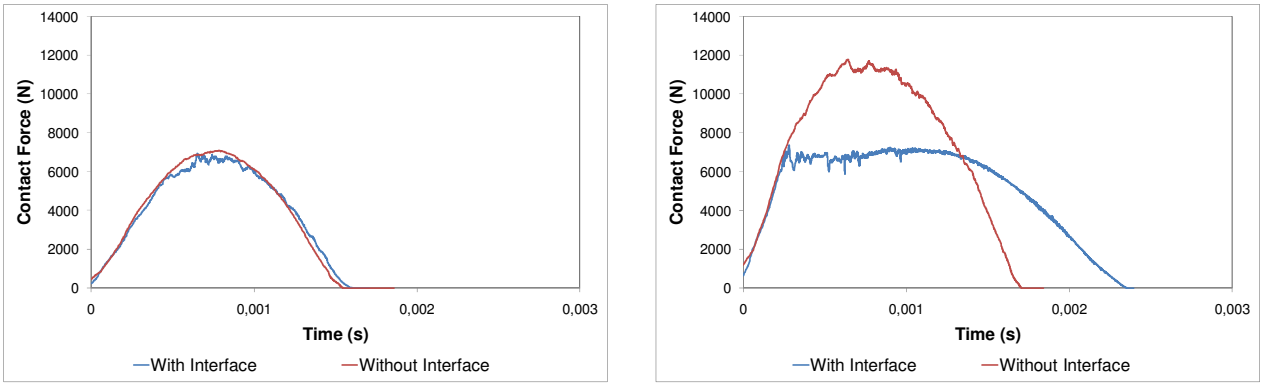

Figure 6. Contact Force time histories for curved plate, κ_3=0.010 mm^{-1}, at impact energies of (a) 4 *J* and (b) 16 *J*

The same behavior can be verified on the Contact Force Histories for the curved plate with κ_3=0.008 mm^{-1}, see Figure 7. This also occurs for all impact energies on curved plate studied herein which presents delamination. The delamination initiates for all energies, aproximatelly, at contact force of 7000 N.

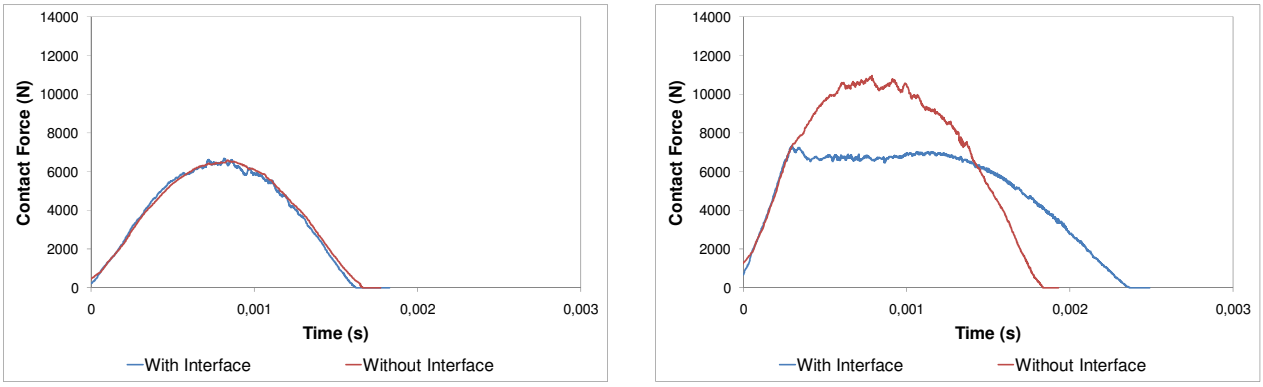

Figure 7. Contact Force time histories for curved plate, κ_2=0.008 mm^{-1}, at impact energies of (a) 4 J and (b) 16 J

The delamination effects can also be verified by the variation of the contact force peak at all impact energies and curvatures studied in this work. Table 3 presents a comparison between the peak force verified on the simulations with and without cohesive layer for the three curvatures analyzed herein. At impact energy of 16 *J* the peak force for plane plate without cohesive layer was about 16% greater than with cohesive layer and for curved plate (κ_3) this difference was about 60%.

Table 3. Percentage of peak force growing for plane and curved plates under delamination effects.

	k_1			k_2			k_3		
Impact Energy (J)	**With Interface (N)**	**Without Interface (N)**	**%**	**With Interface (N)**	**Without Interface (N)**	**%**	**With Interface (N)**	**Without Interface (N)**	**%**
2	3429.33	3368.38	-1.78	4695.39	4601.23	-2.01	**4879.24**	**5375.53**	**10.17**
4	4927.07	4887.61	-0.80	6681.10	6573.60	-1.61	6947.09	7071.81	1.80
6	6042.80	6013.41	-0.49	**7288.29**	**7832.75**	**7.47**	7481.88	8403.42	12.32
8	**6673.19**	**6810.02**	**2.05**	7388.25	8672.40	17.38	7379.37	9135.11	23.79
10	7114.24	7604.14	6.89	7720.21	9343.44	21.03	7400.64	10346.7	39.81
12	7153.97	7990.33	11.69	7310.81	10042.20	37.36	7361.52	10384.5	41.06
16	**7591.87**	**8866.93**	**16.80**	**7337.75**	**10941.40**	**49.11**	**7361.39**	**11791.9**	**60.19**

The damage parameters evolution is presented in Figure 8 for both laminates: (a) plane plate and (b) curved plate, considering the cohesive layer. Figure 8 shows five damage parameter for composite laminates: FFT (Fiber Failure in Tension), FFC (Fiber Failure in Compression), MFT (Matrix Failure in Tension), MFC (Matrix Failure in Compression) and PSF (Plane Shear Failure).The delamination effects on curved plates can also be verified by the failure modes behaviour. The first complete failure of an element occurs at impact energy of 8 *J* by Matrix Failure in Tension for the plane plate and the same failure mode at 6 *J* for curved plate.

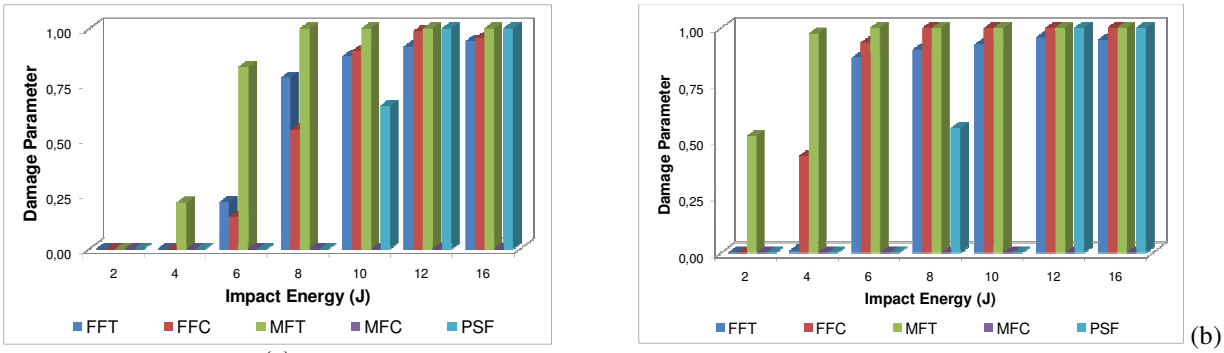

(a) (b)

Figure 8. Damage Parameter for (a) Plane Plate and (b) Curved Plate with cohesive layer

The size of the delaminated area was also greater for the curved plates compared to the plane plate at all impact energies analyzed in this paper. Figure 9 shows the difference between the delaminated area on the plane plate and curved plates for all impact energies studied herein. When delamination occurs the element is deleted from the mesh. The delamination on the plane plate first occurs at 6*J* and on the curved plate at 4 *J*.

	Curved Plate (κ_3)	**Curved Plate (κ_2)**	**Plane Plate (κ_1)**
E=2 *J*	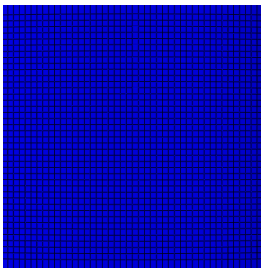	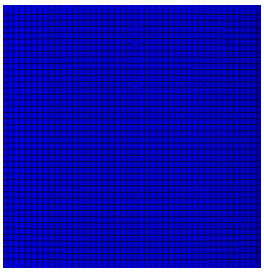	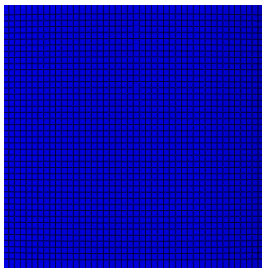

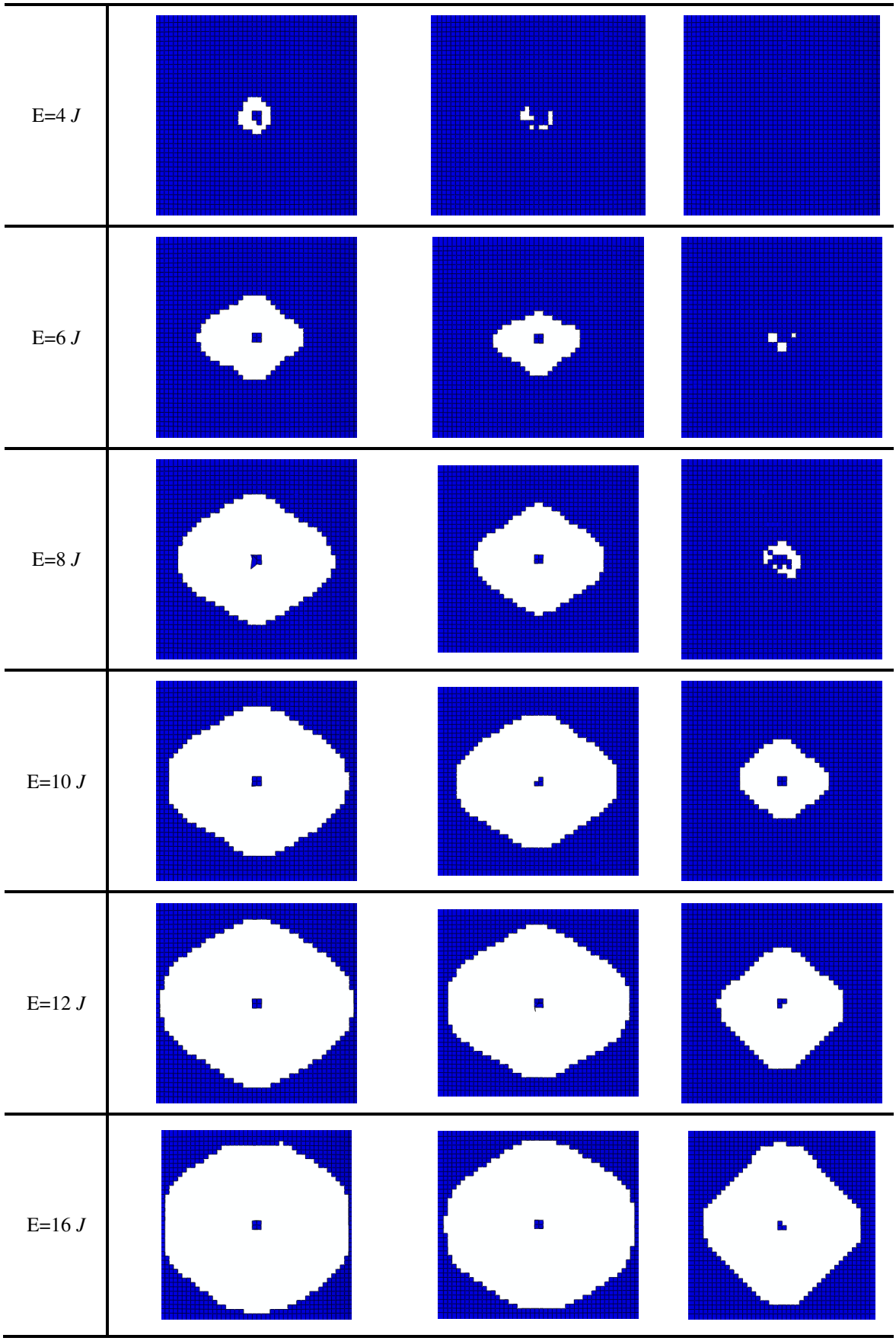

Figure 9. Delaminated area for plane plate and curved plate at all impact energy

6. CONCLUSIONS

In this paper, plane and curved plates were studied at different impact energies using solid elements and considering the delamination effects. The results obtained in terms of "Contact Force Histories", "Dissipated Energies", "Failure Modes" and "Delaminated Area" indicated that curved plates were more susceptible to the effects of delamination than plane plates. Even for low impact energies the curved plate presents a delaminated area greater then on plane plate, at all impact energies studied. For both cases, plane and curved plates, since the delamination ocurs the damage grows at all impact energies. However, the delaminated area and damage modes evolution was more pronounced for curved plates than plane plate.

Comparing the delaminated area evolution for each curvature at all impact energies studied herein, it can be concluded that higher curvatures lead to more pronounced damage and delamination extent when composite laminates are subject to low velocity impact loading. This indicate that delamination plays an important rule on the impact behavior of composite curved plates and such effect must be taken into account in the design and analysis of composite structures.

7. ACKNOWLEDGMENTS

The authors acknowledge the financial support received for this work from Coordenação de Aperfeiçoamento de Pessoal de Nível Superior (Capes), the Fundação de Amparo a Pesquisa do Estado de São Paulo (Fapesp), contract number 2006/06808-6, CNPq Grants 305601/2007-5 and 303287/2009-8.

REFERENCES

Sun C. T., Jih C. J. “Quasi-static modeling of delamination crack propagation in laminates subjected to low-velocity impact”. Composites Science and Technology; 1995; Vol. 54; pp 185-191.

Yokoyama N. O., Donadon M. V., de Almeida S. F. M. “A numerical study on the impact resistance of composite shells using na energy based failure model”. Composite Strucutures; 2010; Vol 93; pp 142-152.

Gning P. B., Tarfaoui M., Collombet F., Riou L., Davies P. “Damage development in thick composite tubes under impact loading and influence on implosion pressure: experimental observations”. Composites: Part B; 2005; Vol. 36; pp 306-318.

Olsson R. “Analytical model for delamination growth during samall mass impact on plates”. International Journal of Solids and Structures; 2010; Vol. 47; pp 2884-2892.

Donadon M. V., de Almeida S. F. M., Arbelo M. A., de Faria A. R. “A three-dimensional ply failure model for composite structures”. International Journal of Aerospace Engineering; 2009; Article ID 486063; doi: 10.1155 /2009 /486063.

Puck A. and Schürmann H. “Failure analysis of FRP laminates by means of physically based phenomenological models” Composites Science and Technology; 1998; Vol. 58; pp 1045–1067.

S. Pinho, L. Iannucci, and P. Robinson, “Physically-based failure models and criteria for laminated fibre reinforced composites with emphasis on fibre kinking—part I: development,”Composites Part A, vol. 37, no. 1, pp. 63–73, 2006.

S. Pinho, P. Robinson, and L. Iannucci, “Physically-based failure models and criteria for laminated fibre reinforced composites with emphasis on fibre kinking: part II: FE implementation,” Composites Part A, vol. 37, no. 5, pp. 766–777, 2006.

Donadon M.V., Almeida S. F. M. “A contact-logic for mixed-mode modelling in composite laminates”, To be submitted to International Journal of Aerospace Engineering; 2010.

RESPONSIBILITY NOTICE

The authors are the only responsible for the printed material included in this paper.